Compositional effects on the optical and thermal properties of potassium aluminophosphate glasses

E.T.Y. Lee* and E.R.M. Taylor

Optoelectronics Research Centre,

University of Southampton, Highfield, Southampton SO17 1BJ, UK

The K_2O-Al_2O_3-P_2O_5 glass system has been examined and various compositions have been melted. Their optical and thermal properties have been measured to assess their potential for athermalisation. The addition of alumina (Al_2O_3) increases the refractive index (n) and glass transition temperature (T_g) and decreases the thermal expansion coefficient (α), consequently leading to positive thermo-optic coefficient (dn/dT). In addition to thermal expansion, polarisability of the glass also affects dn/dT. Generally, glasses must exhibit negative dn/dT to counter thermal expansion, in order to have potential application in athermalisation.

PACS : 78.20.Nv; 65.60.+a;61.43.Fs; 42.70.C

***Keywords** : Athermal, Thermal expansion coefficient, Thermo-optic coefficient, Phosphate glasses*

1. Introduction

Lightwave devices such as gratings have a problem in that the central wavelength of such devices is sensitive to changes in temperature. This is caused by the devices' optical path

* *Corresponding author*
E-mail address: tyl@orc.soton.ac.uk
Tel.: +44 023 8059 4530; Fax: +44 023 8059 3149

length dependence on temperature [1-5]. Thus, the use of such devices in Wavelength Division Multiplexing (WDM) systems compromises the efficiency of the systems. Due to the limitations of passive temperature control units [3-5], an athermal waveguide, being inherently insensitive to temperature, is an ideal choice to overcome this problem of thermal fluctuation.

Potassium aluminophosphate (KAP) glasses are ideal candidates for athermalisation because, to begin with, pure phosphate glasses exhibit negative thermo-optic coefficient, -92.2×10^{-6}/K [6], which is required to counter the effect of thermal expansion. Different modifying cations can be added to phosphate glasses to change their properties to meet various optical and thermal requirements. Potassium has been chosen because from among the various metaphosphate glasses, potassium phosphate exhibits the highest magnitude of negative *dn/dT* [6]. Although aluminophosphate exhibits positive *dn/dT*, aluminium has been added to improve the chemical durability of the glasses [7,8].

In order to achieve athermalisation, the change in optical path length (*dS*) of a homogeneous bulk material with temperature must be zero. This is defined as

$$\frac{1}{L}\left(\frac{dS}{dT}\right)=n\alpha+\frac{dn}{dT} \qquad (1)$$

It follows then that in order to obtain *dS/dT* equal to 0 in a single material, we need to satisfy the following athermal condition:

$$\frac{dn}{dT}=-n\alpha \qquad (2)$$

A thorough analysis of the principle of athermalisation had been carried out elsewhere [9]. As glasses exhibit positive α values, dn/dT must be negative to satisfy equation (2). As shown in equation (2), n, α and dn/dT of a particular glass must be measured in order to determine the potential of a glass for athermalisation.

The main aim of this paper is to assess the optical and thermal properties of KAP glasses at the ultraphosphate and polyphosphate compositions, with the view for potential athermalisation applications, and examine how different compositions affect these properties. A detailed study of the properties of KAP glasses at the stoichiometric metaphosphate composition had been carried out and reported elsewhere [9].

2. Experimental

2.1 Glass preparation

Various compositions of potassium aluminophosphate (KAP) glasses were prepared with O/P ranging approximately between 2.8 and 3.1 using the appropriate mixtures of high purity powder of K_2CO_3, $Al(OH)_3$ and P_2O_5. The mixtures were melted in covered silica crucibles at temperatures between 1050°C and 1450°C, depending on the glass compositions. After 90 minutes of melting, the melts were then cast into a graphite mould to form rectangular samples. They were then annealed for 60 minutes near the glass transition temperature (T_g) and finally cooled at a rate of 0.5°C/min to room temperature.

2.2 Property measurements

The refractive index of the glasses were measured at room temperature using an Abbē '60' refractometer at the sodium D-line (λ=589.3nm), to within an accuracy of ±0.0005. This equipment makes use of the total internal reflection phenomenon to measure the refractive index.

The thermal properties were measured using a thermomechanical analyser (Perkin Elmer TMA7) to measure the α in the temperature range of 50-300°C and a differential thermal analyser (Perkin Elmer DTA7) to measure the T_g. The heating rate used were 5°C/min and 10°C/min for α and T_g respectively. The onset of crystallisation, T_x, and peak crystallisation, T_p, temperatures were also determined during the T_g measurement.

A 3-step polishing procedures using three different solutions containing 9 μm alumina powder, 3 μm alumina powder and 0.125 μm silica particles respectively were then carried out on the glass samples. *dn/dT* measurements were performed on these polished glass samples using the interferometer set-up as shown schematically in Figure 1. The glass sample is held by two aluminium plates inside the furnace. The front plate has an opening to allow for light to reach the sample and is spring loaded to allow for sample expansion while the back plate is fixed in place. The measurements were carried out in the temperature range of 20-100°C at a rate of 40°C/hour. The sinusoidal interference fringe pattern obtained, due to interference of the light reflected from the front and back

surfaces of the glass sample, was then used to obtain the thermo-optic coefficient, *dn/dT* using the following equation [10-11]:

$$\frac{dn}{dT} = \left(\frac{\lambda}{2l\Delta T}\right) - n\alpha \qquad (3)$$

where λ is the laser wavelength (λ = 632.8nm), l is the sample thickness (typically l = 10 mm), n is the refractive index, α is the thermal expansion coefficient and ΔT is the measured temperature difference between adjacent peaks or troughs from interferometry. An average *dn/dT* value is taken and reported as the ΔT parameter does not vary significantly over the temperature range of 20-100°C.

3. Results

Tables 1 to 4 show the compositions of the various KAP glasses of the K_2O-Al_2O_3-P_2O_5 system studied, along with their associated properties. Table 1 shows the compositions of glasses where P_2O_5 has been fixed at 65 mol% while varying the mol% of both K_2O and Al_2O_3 (designated as group 1). Tables 2 and 3 show the compositions of glasses where K_2O has been fixed at 20 mol% (designated as group 2) and Al_2O_3 fixed at 15 mol% (designated as group 3) respectively. The single metaphosphate composition in the tables had previously been studied along with other metaphosphate compositions [9] and is included as a standard reference. The networks of the phosphate glasses are classified as either ultraphosphate, metaphosphate or polyphosphate in the tables, depending on the O/P ratio as set by the glass compositions.

The refractive index of the glasses is shown in Figures 2a and 2b. An increase in the Al_2O_3 mol% increases the refractive index of the groups 1 and 2 glasses while for the group 3 compositions where the Al_2O_3 is fixed at 15 mol%, an increase in the K_2O mol% decreases the refractive index.

Figures 3 and Figures 4 show the variation of thermal properties of the glasses as a function of Al_2O_3 mol% for groups 1 and 2 and K_2O mol% for Group 3 glasses. The glass transition temperature (T_g) increases while the thermal expansion coefficient (α) decreases as the alumina content increases for the groups 1 and 2 glasses, as shown in Figures 3a and 4a. These results are reversed for the group 3 glasses when K_2O replaces P_2O_5 with Al_2O_3 fixed (Figures 3b and 4b).

Figures 5a and 5b show the compositional effects on the thermo-optic coefficient (*dn/dT*) of the glasses. The addition of alumina changes *dn/dT* to a positive value. However, for the group 3 glasses, the substitution of K_2O for P_2O_5 leads to a negative value.

Table 4 shows the athermalisation parameters of the KAP glasses. The $n\alpha$ values are calculated from the results in Tables 1 to 3 while the *1/L(dS/dT)* values are determined using equation (1). Silica has been included for comparison.

4. Discussion

The refractive index increases for the groups 1 and 2 KAP glasses as the Al_2O_3 content increases, which concurs with literature [7,9,12], and decreases for the group 3 glasses as the K_2O content increases. The refractive index change occurs due to the ionic refractivity difference between K^+, Al^{3+} and P^{5+} as well as the molar volume change when different cations are added. The refractive index of a particular glass is dependent on the polarisability and molar volume of the glass, as given by the Lorentz-Lorenz equation [13]:

$$\frac{n^2 - 1}{n^2 + 2} = \frac{4}{3}\frac{\pi N_a P_e}{V_m} \qquad (4)$$

where n is the refractive index, N_a is the Avogadro's number, P_e is the polarisability and V_m is the molar volume.

When cations are added to phosphate glasses, the modifiers depolymerise the phosphate network, thus diminishing the cross-linking of the phosphate glass network to create a more open structure. Also, the addition of cation modifiers causes the glass structure to expand to accommodate the cations at interstitial sites. Therefore this increase in molar volume, having a considerable effect compared to any polarisability effect, leads to the decrease of the refractive index of the glasses. However, when a high modifier field strength (defined as the ratio of the ion valence to the square of the bond distance between the ion and oxygen (z/a^2) [14]) cation, such as Al^{3+}, is added, the cation forms strong P-O-P bonds [15] between the phosphate chains. This strengthening effect is considered by Kreidl *et al.* [16], whose model suggests that Al^{3+} cross-links the

phosphate chains, resulting in an increase in structural polymerisation. This creates a more rigid network and causes a decrease in the molar volume, leading to higher refractive index. In addition to the above mentioned structural changes, there is another effect affecting the refractive index of the group 1 glasses. K^+ has a larger ionic radius and smaller polarisability effect, due to its more ionic nature, compared to Al^{3+}. Hence, the substitution of Al_2O_3 for K_2O with fixed mol% of P_2O_5 reduces the molar volume of the glass, besides increasing the polarisability of the glass. This leads to a higher refractive index, according to equation (4). This trend agrees with our results for the group 1 glasses.

Based on the above discussions, therefore, the substitution of Al_2O_3 for either K_2O or P_2O_5 increases the refractive index while the substitution of K_2O for P_2O_5 decreases the refractive index. Such observations have been previously noted for sodium aluminophosphate glasses [7].

The glass transition temperature increases and the thermal expansion coefficient decreases as the alumina content increases for the groups 1 and 2 glasses, despite the depolymerisation of the phosphate glass network from ultraphosphate, through metaphosphate to polyphosphate. This variation of the thermal properties with glass compositions are consistent with the effects of modifier field strength. Al^{3+} has a higher field strength than K^+ and therefore forms stronger bridging bonds between the phosphate chains. This strengthening effect of Al^{3+} on the glass structure increases the T_g and reduces the α of the glass, as evident in Tables 1 and 2 and Figs. 3a and 4a. However,

these trends are reversed for the group 3 glasses when the K_2O content increases with the alumina content fixed due to the low field strength of K^+. This is because the addition of K^+ breaks up and depolymerises the phosphate cross-linked network, thus weakening the bond strength of the glass structure. The weakened bonds cause a decrease in T_g and an increase in α. This is consistent with the results shown in Table 3 and Figs. 3b and 4b.

The variation of α and *dn/dT* as a function of $Al(PO_3)_3$ mol fraction are shown in Figures 6-8, which include the α and *dn/dT* results of the potassium alumino-metaphosphate glasses for comparison [9]. The figures show that a decrease in α results in a positive *dn/dT* value. The results for the groups 1, 2 and 3 glasses follow a similar curve as the metaphosphate glasses. This suggests that the phosphate glass networks gradually and systematically changes from a network of cross-linked phosphate tetrahedra to a network of metaphosphate chains of phosphate tetrahedra with the addition of either Al_2O_3 or K_2O and that any deficiency in P_2O_5 (polyphosphates) or excess P_2O_5 (ultraphosphates) does not affect α and *dn/dT* abnormally. It also shows that in order to obtain negative *dn/dT*, one needs approximately $\alpha > 10\times10^{-6}/°C$.

The link between α and *dn/dT* can be established from the Lorentz-Lorenz equation, as shown below with the approximation of $(d(lnV)/dT \sim 3\alpha)$.

$$\frac{dn}{dT} = A\left[\frac{d(\ln P_e)}{dT} - 3\alpha\right] \qquad (5)$$

where $A=[(n^2-1)(n^2+2)/6n]$, P_e is the polarisability and α is the thermal expansion coefficient.

Equation (5) shows that apart from α, P_e also has an effect on *dn/dT*. As discussed earlier, an increase in the groups 1 and 2 alumina content and a decrease in the group 3 K_2O content result in higher polarisability due to a reduction in the aluminium co-ordination number. This effect, coupled with decreased α values, leads to a positive *dn/dT* value, according to equation (5), which agrees with the results obtained.

Equation (5) can also be represented in another form by assuming that polarisability is increased by an increase in the inter-ionic distance. This leads to equation (6) below, with the assumption of $(d(\ln P_e)/dT=[\partial(\ln P_e)/\partial(\ln r)]_T[d(\ln r)/dT])$ where $\alpha=[d(\ln r)/dT]$:

$$\frac{dn}{dT} = A(\gamma - 3)\alpha \qquad (6)$$

where γ is the change in polarisability due to a change in inter-ionic distance $(\gamma=\partial(\ln P_e)/\partial(\ln r)_T)$, P_e is the polarisability, r is the inter-ionic distance and α is the thermal expansion coefficient.

Figure 9 shows the relationship of *dn/dT* on α, which has a linear dependence. This linear dependence is valid as n and α are linear functions of the Al_2O_3 content (Figures 2(a) and 4(a)) and K_2O content (Figures 2(b) and 4(b)) as well as A being a linear function of n (Figure 10). Figure 9 represents a semi-empirical fit for the composition of KAP glasses exhibiting $1.469 \leq n \leq 1.519$. This allows the *dn/dT* of any KAP glasses within this range to be estimated if the α and n values are known.

As equation (2) shows, the positive values of α require that glasses must exhibit negative *dn/dT* to counter the effect of expansion in order to fulfil the athermal condition. From Table 4, we can see that a number of samples exhibit negative *dn/dT*.

On their own, the glasses studied in this work are not athermal as their respective *1/L(dS/dT)* values are not zero as shown in Table 4, with silica being slightly better compared to the potassium aluminophosphate glasses. However it is possible to produce athermal waveguides based on these glasses, where we need to employ a multi-layer system approach with the use of suitable substrates of lower α values [2-5]. Using this method, the substrate thermal expansion coefficient, α_{sub}, is more critical than the expansion of the core layer, α_{core}, in the overall device because of the substrate's thicker dimension. Therefore, equation (1) of $1/L(dS/dT) = n\alpha + dn/dT$ for bulk glass can be modified to the following equation for waveguides:

$$\frac{1}{L}\left(\frac{dS}{dT}\right) = n_{eff}\,\alpha_{sub} + \left(\frac{dn}{dT}\right)_{eff} \qquad (7)$$

where n_{eff} is the effective refractive index and $(dn/dT)_{eff}$ is the effective thermo-optic coefficient of the waveguide. The principles and realisation of such athermal waveguides is under study.

5. Conclusions

Different compositions of potassium aluminophosphate (KAP) glasses, encompassing ultraphosphates and polyphosphates have been assessed. The substitution of Al_2O_3 for

either K_2O or P_2O_5 strengthens the glass structural network, resulting in lower thermal expansion coefficients and consequently positive thermo-optic coefficients. For low field strength modifier, the progression from ultraphosphate to polyphosphate weakens the glass network, resulting in higher thermal expansion coefficients and consequently negative thermo-optic coefficients. Ultraphosphate and polyphosphate compositions do not affect α and *dn/dT* abnormally, suggesting a gradual change in structural network. *dn/dT* and α are inter-dependent and a value of α>10×10-6/°C is required to obtain negative dn/dT. Glasses with negative *dn/dT* have been achieved and this shows that phosphate glasses are promising candidates for athermal waveguide development, via a multi-layer system with the use of suitable low expansion substrates from the same family of glass.

Acknowledgements

The authors would like to acknowledge the financial support of the Engineering and Physical Sciences Research Council (EPSRC) under EPSRC/PHOTON/GR/M98876 project 'Physical-Layer High-Speed Optoelectronics for Tomorrow's Optical Networks'.

References

[1] A. Sakamoto, T. Matano, H. Takeuchi, IEICE Trans. Electron. E83-C (9) (2000) 1441.

[2] K. Kintaka, J. Nishii, H. Nishiyama, Y. Kawamoto, A. Sakamoto, J. Lightwave Tech. 21 (3) (2003) 831.

[3] Y. Kokubun, N. Funato, M. Takizawa, IEEE Photon. Tech. Lett. 5 (11) (1993) 1297.

[4] Y. Kokubun, S. Yoneda, H. Tanaka, Electron. Lett. 32 (21) (1996) 1998.

[5] Y. Kokubun, S. Yoneda, S. Matsuura, Electron. Lett. 34 (4) (1998) 367.

[6] W. Vogel, in: D.R. Uhlmann and N.J. Kreidl (Eds), Optical Properties of Glass, The American Ceramic Society Inc., OH, 1991, pp. 18-19.

[7] R.K. Brow, J. Am. Ceram. Soc. 76 (1993) 913.

[8] Y. Lin, Y. Zhang, W. Huang, K. Lu, Y. Zhao, J. Non-Cryst. Solids 112 (1989) 136.

[9] E.T.Y. Lee, E.R.M. Taylor, Presented at the 'Glass & Optical Materials Division Fall 2003 Meeting, Corning (NY), 12-15 October 2003 (Paper : GOMD-S1-29a-2003).

[10] J.M. Jewell, C. Askins, I.D. Aggarwal, Appl. Opt. 30 (25) (1991) 3656.

[11] R.J. Harris, G.T. Johnston, G.A. Kepple, P.C. Krok, H. Mukai, Appl. Opt. 16 (2) (1977) 436.

[12] E. Metwalli, R.K. Brow, J. Non-Cryst. Solids 289 (2001) 113.

[13] M. Born and E. Wolf, Principles of Optics, Ch 2, Pergamon Press, Oxford, 1984.

[14] A. Dietzel, Z. Elektrochem. 48 (1942) 9.

[15] A. Eisenberg, H. Farb and L.G. Cool, J. Polym. Sci.: PartA-2 4 (1966) 855.

[16] N.J. Kreidl and W.A. Weyl, J. Am. Ceram. Soc. 24 [11] (1941) 372.

Figure captions

Fig. 1 Interferometer set-up to measure *dn/dT*

Fig. 2a Refractive index of groups 1 and 2 KAP glasses

Fig. 2b Refractive index of group 3 KAP glasses

Fig. 3a Glass transition temperature (T_g) of groups 1 and 2 KAP glasses

Fig. 3b Glass transition temperature (T_g) of group 3 KAP glasses

Fig. 4a Thermal expansion coefficient (α) of groups 1 and 2 KAP glasses

Fig. 4b Thermal expansion coefficient (α) of group 3 KAP glasses

Fig. 5a Thermo-optic coefficient (*dn/dT*) of groups 1 and 2 KAP glasses

Fig. 5b Thermo-optic coefficient (*dn/dT*) of group 3 KAP glasses

Fig. 6 α and *dn/dT* of KAP metaphosphate and group 1 glasses as a function of $Al(PO_3)_3$ mol fraction

Fig. 7 α and *dn/dT* of KAP metaphosphate and group 2 glasses as a function of $Al(PO_3)_3$ mol fraction

Fig. 8 α and *dn/dT* of KAP metaphosphate and group 3 glasses as a function of $Al(PO_3)_3$ mol fraction

Fig. 9 *dn/dT* of KAP glasses as a function of α

Fig. 10 Dependence of A on n

Fig. 1 Interferometer set-up to measure *dn/dT*

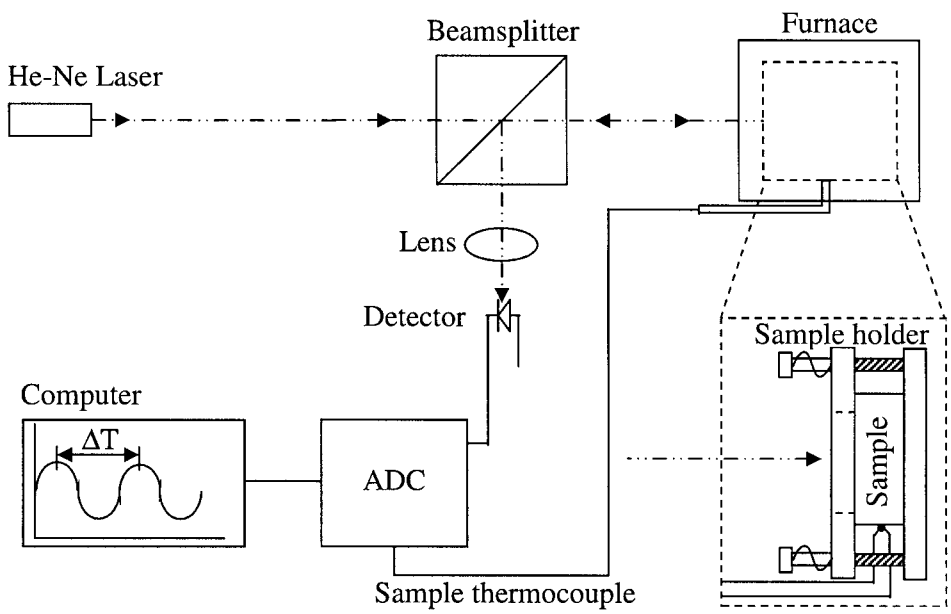

Fig. 2a Refractive index of groups 1 and 2 KAP glasses

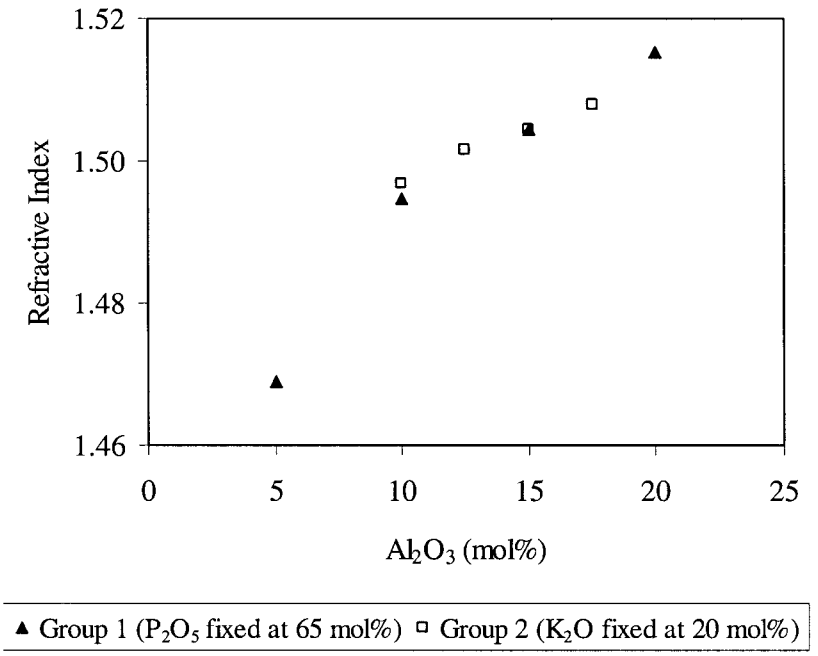

Fig. 2b Refractive index of group 3 KAP glasses

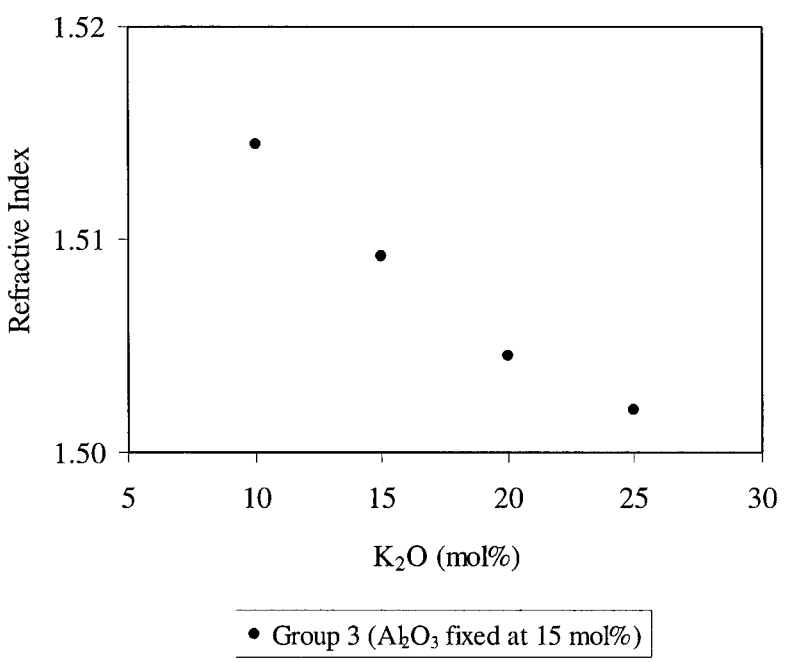

Fig. 3a Glass transition temperature (T_g) of groups 1 and 2 KAP glasses

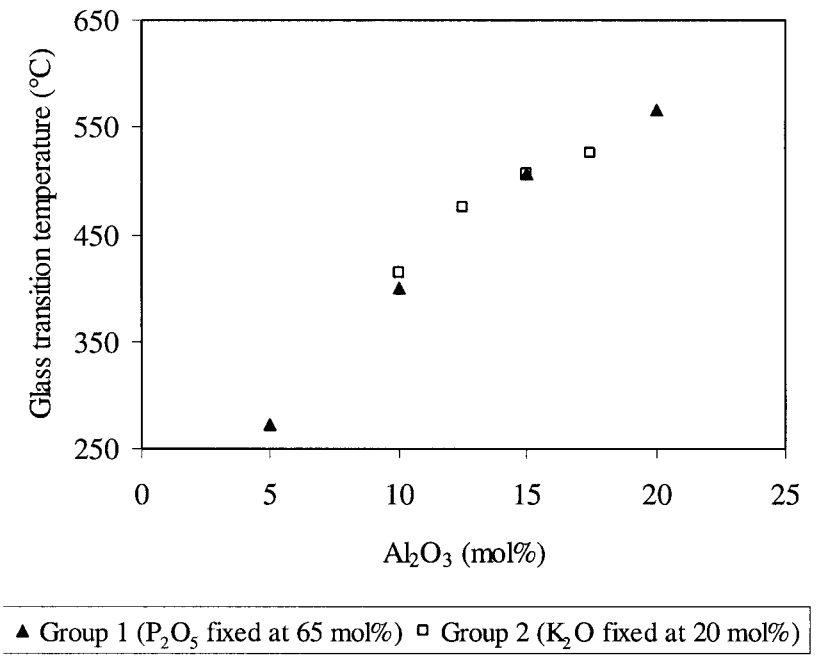

Fig. 3b Glass transition temperature (T_g) of group 3 KAP glasses

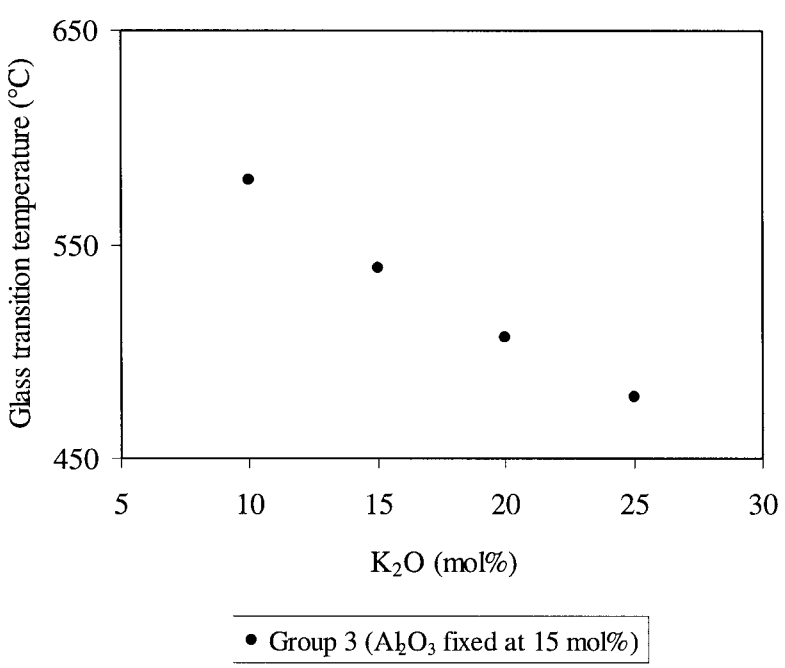

Fig. 4a Thermal expansion coefficient (α) of groups 1 and 2 KAP glasses

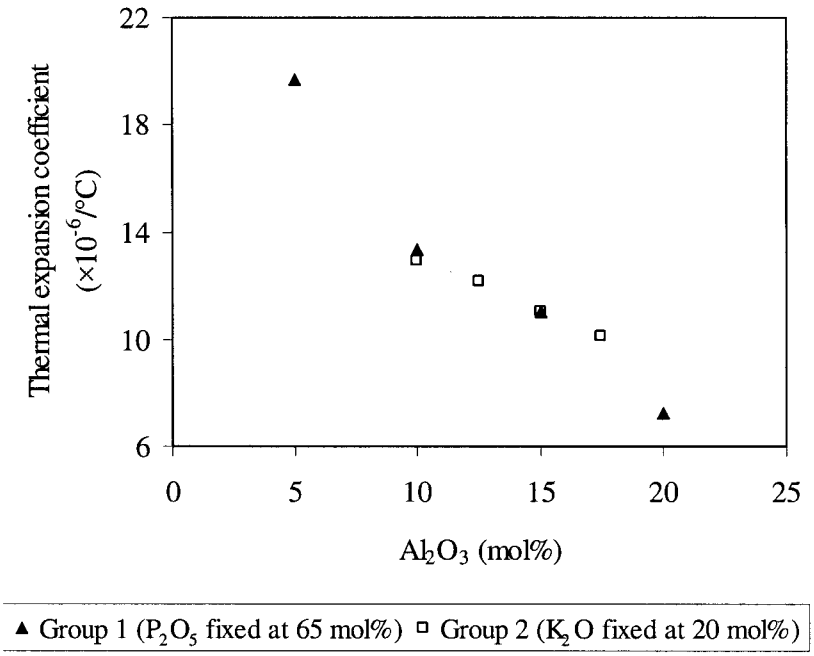

Fig. 4b Thermal expansion coefficient (α) of group 3 KAP glasses

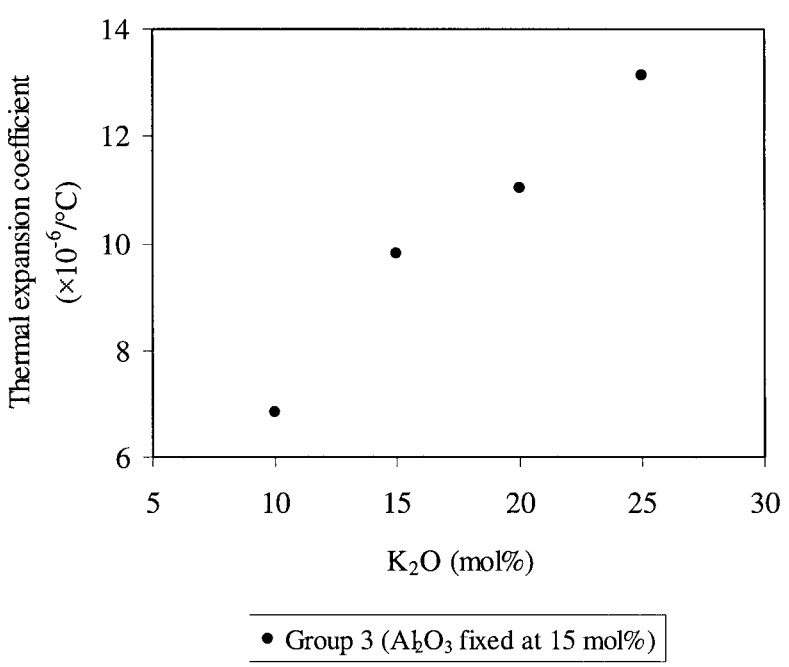

Fig. 5a Thermo-optic coefficient (*dn/dT*) of groups 1 and 2 KAP glasses

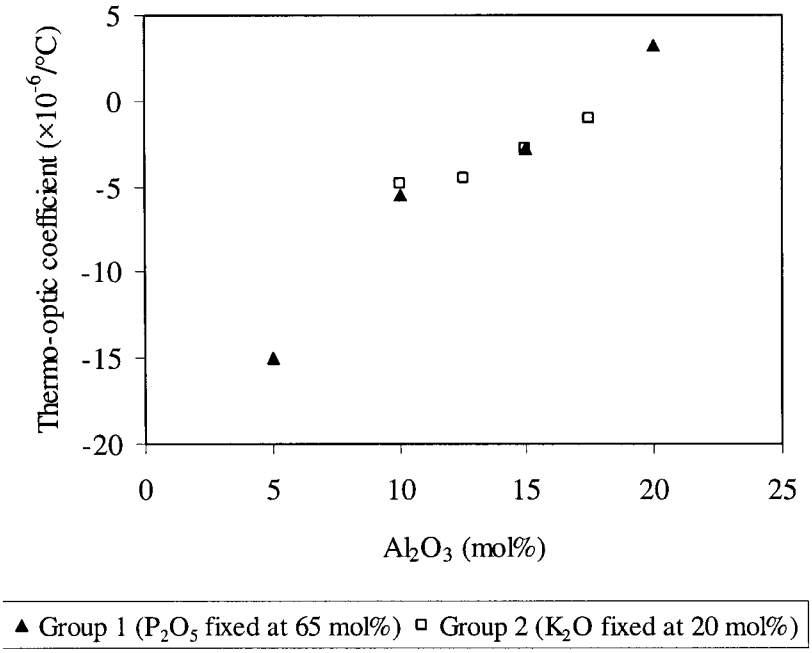

Fig. 5b Thermo-optic coefficient (*dn/dT*) of group 3 KAP glasses

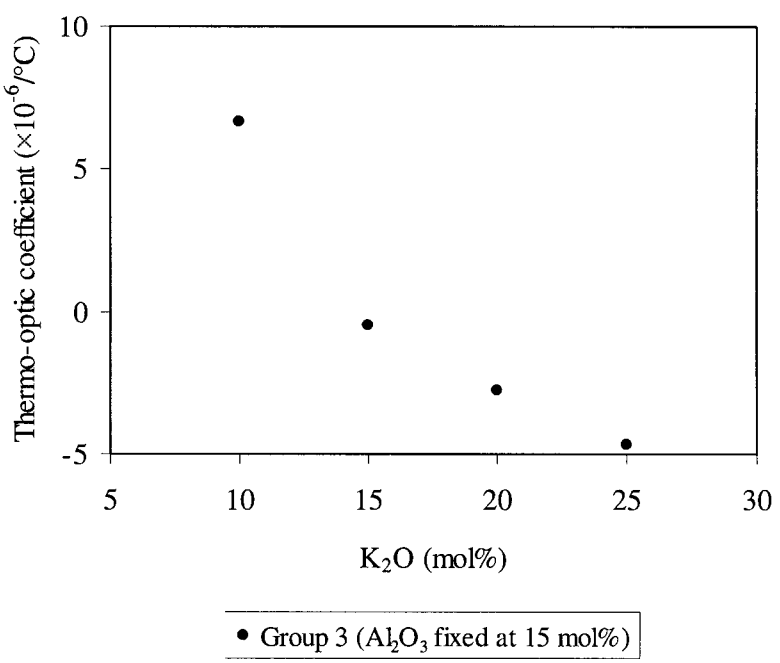

Fig. 6 α and *dn/dT* of KAP metaphosphate and group 1 glasses as a function of $Al(PO_3)_3$ mol fraction

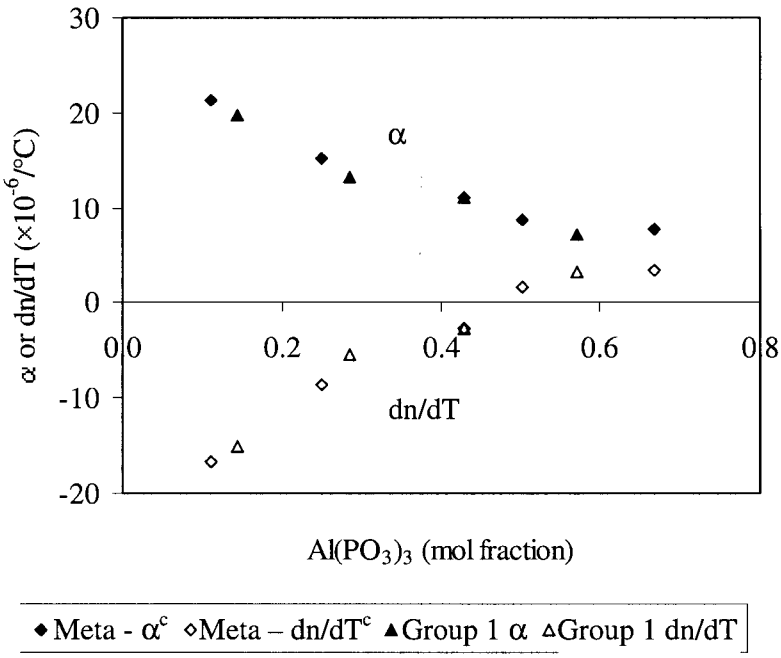

[c] Ref[9]

Fig. 7 α and *dn/dT* of KAP metaphosphate and group 2 glasses as a function of $Al(PO_3)_3$ mol fraction

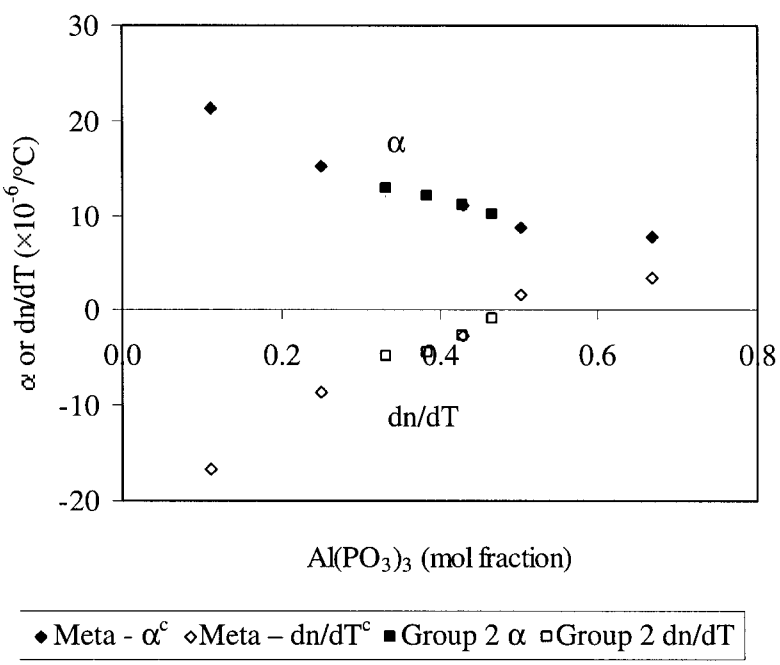

[c] Ref[9]

Fig. 8 α and *dn/dT* of KAP metaphosphate and group 3 glasses as a function of $Al(PO_3)_3$ mol fraction

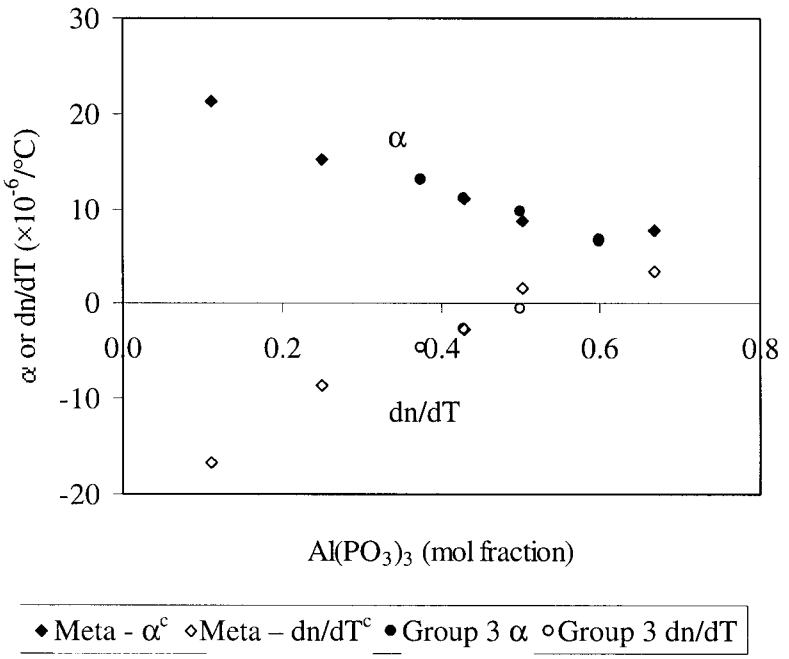

[c] Ref[9]

Fig. 9 *dn/dT* of KAP glasses as a function of α

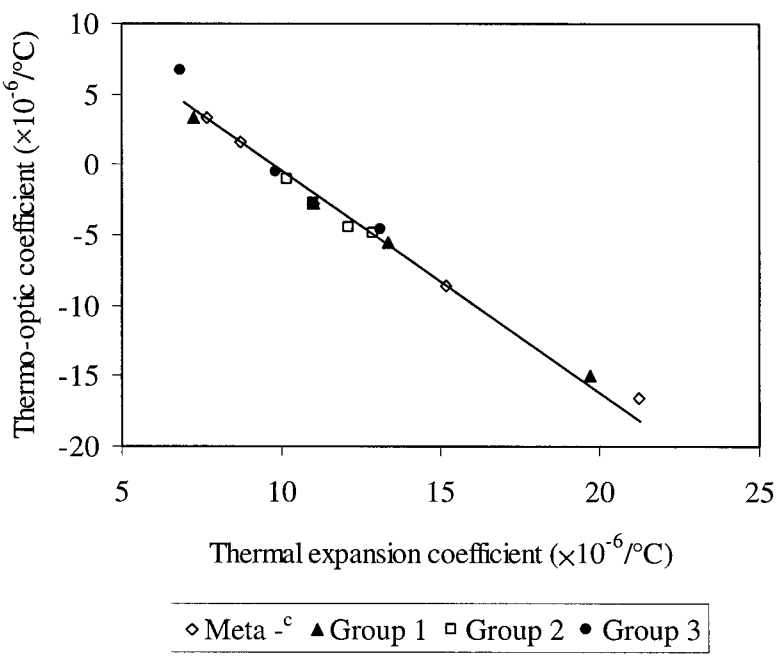

[c] Ref[9]

Fig. 10 Dependence of A on n

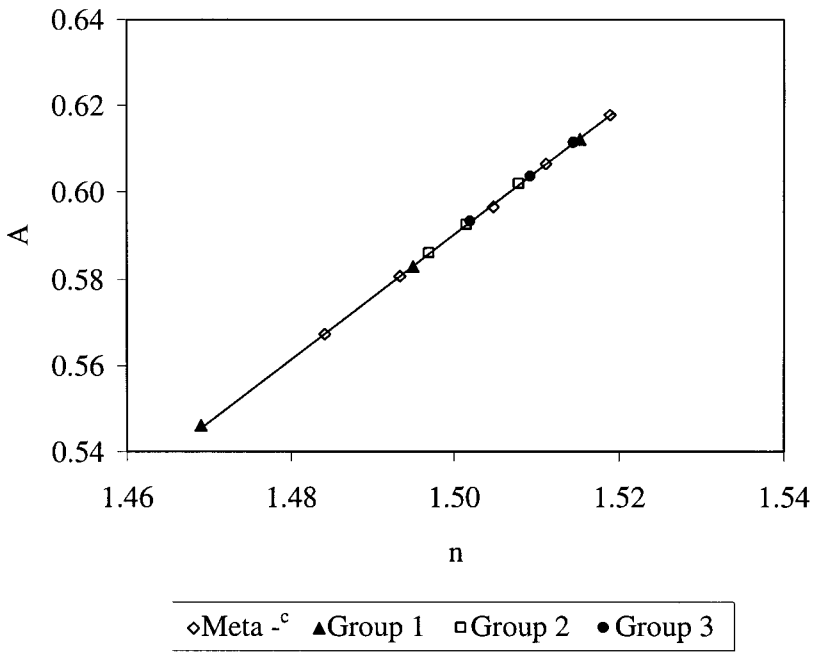

[c] Ref[9]

Table 1 Properties of KAP glasses, with phosphorus oxide fixed at 65 mol%

Composition (mol%)				n	T_g (°C)	T_x (°C)	T_p (°C)	α ($\times 10^{-6}$/°C)	*Phosphate*
Sample	K_2O	Al_2O_3	P_2O_5						
1a	30	5	65	1.469	272	558	670	19.70	Ultra-
1b	25	10	65	1.495	400	618	782	13.34	Ultra-
1c[a]	20	15	65	1.505	507	759	849	11.02	Meta-
1d	15	20	65	1.515	567	814	882	7.23	Poly-

[a] Ref[9]

Table 2 Properties of KAP glasses, with potassium oxide fixed at 20 mol%

Composition (mol%)				n	T_g (°C)	T_x (°C)	T_p (°C)	α ($\times 10^{-6}$/°C)	*Phosphate*
Sample	K_2O	Al_2O_3	P_2O_5						
2a	20	10	70	1.497	415	755	800	12.91	Ultra-
2b	20	12.5	67.5	1.502	475	736	793	12.15	Ultra-
2c[a]	20	15	65	1.505	507	759	849	11.02	Meta-
2d	20	17.5	62.5	1.508	526	702	798	10.15	Poly-

[a] Ref[9]

Table 3 Properties of KAP glasses, with aluminium oxide fixed at 15 mol%

Composition (mol%)				n	T_g (°C)	T_x (°C)	T_p (°C)	α ($\times 10^{-6}$/°C)	*Phosphate*
Sample	K_2O	Al_2O_3	P_2O_5						
3a	10	15	75	1.515	580	>900	>900	6.84	Ultra-
3b	15	15	70	1.509	539	749	>850	9.80	Ultra-
3c[a]	20	15	65	1.505	507	759	849	11.02	Meta-
3d	25	15	60	1.502	479	704	748	13.13	Poly-

[a] Ref[9]

Table 4 Athermalisation parameters of KAP glasses

Composition (mol%)				dn/dT ($\times 10^{-6}$/°C)	$n\alpha$ ($\times 10^{-6}$/°C)	$1/L(dS/dT)$ ($\times 10^{-6}$/°C)
Sample	K_2O	Al_2O_3	P_2O_5			
1a	30	5	65	-14.99	28.94	13.95
1b	25	10	65	-5.48	19.94	14.46
1c[a]	20	15	65	-2.76	16.59	13.83
1d	15	20	65	+3.30	10.95	14.25
2a	20	10	70	-4.83	19.33	14.50
2b	20	12.5	67.5	-4.45	18.25	13.80
2c[a]	20	15	65	-2.76	16.59	13.83
2d	20	17.5	62.5	-0.99	15.31	14.32
3a	10	15	75	+6.63	10.35	16.98
3b	15	15	70	-0.47	14.79	14.32
3c[a]	20	15	65	-2.76	16.59	13.83
3d	25	15	60	-4.66	19.72	15.06
Silica[b]				+10.4	0.80	11.20

[a] Ref[9], [b] Ref [6]